Conceptual Research and Verification of a Single-stage High-precision Pointing Technology

Yong-Gang Du (duygemail@163.com)
Lanzhou Institute of Physics https://orcid.org/0000-0003-1457-9984
Yu-Lin Wang
Lanzhou Institue of physics
Xue-song Wang
Lanzhou Institute of Physics
Chun-Jie Yan
Lanzhou institue of Physics

Original Article

Keywords: Concept ,High precision , Pointing , Single-stage control , Verification

Posted Date: November 15th, 2021

DOI: https://doi.org/10.21203/rs.3.rs-1046419/v1

ORIGINAL ARTICLE

Conceptual Research and Verification of a Single-stage High-precision Pointing Technology

Yong-Gang Du[1] • Yu-Lin Wang[1] • Xue-Song Wang[1] • Chun-Jie Yan[1,2]

Received June xx, 201x; revised February xx, 201x; accepted March xx, 201x

Abstract: High-precision pointing plays a critical role in optical equipment and laser communication systems. In order to reach the level of sub mrad for pointing accuracy, a two-stage pointing technology is currently widely used. However, this results in significant technical complexity. Therefore, the realization of a high-precision pointing technology under single-stage control is highly challenging. In this study, we find that erase the floating errors of the middle link of the mechanism can effectively improve the pointing accuracy. Based on this assumption, we propose the concept of a single-stage high-precision pointing technology and also establish its mathematical model of drive and an error elimination algorithm. Using modern computer technology, we study the working principle of this single-stage high-precision pointing technology in detail. We also build a prototype and test its performance. The test results show that the uniaxial error of the prototype is no greater than 0.004°, while its spatial synthetic error is no greater than 0.006° and the stability time is less than 100 ms. The test results show that this concept is completely feasible. It is also found that the accuracy of the pointing system can further be improved when the vibration is suppressed, which also represents an important concept for further research. We anticipate that an ultra-high-precision pointing system with single-stage control will be established in the near future.

✉ Yong-Gang Du

duygemail@163.com

1 Lanzhou Institute of physics, Lanzhou, 730000, China

2 National Key Laboratory of Vacuum Technology and Physics, Lanzhou, 730000, China

Keywords: Concept •High precision • Pointing • Single-stage control • Verification

1 Introduction

As a key technology of optical equipment for aerospace, high-precision pointing technology is widely used in the fields of aviation and aerospace. Furthermore, even with the rapid development of laser communication systems in recent years, there is still a strong demand for this technology in civil applications.

In the aerospace field, the optical systems of various spacecraft have very stringent requirements for pointing technology, for example, the James Web telescope requires a pointing accuracy that can reach 0.004" [1], while the Large UV Optical Infrared Telescope (LUVOIR, America) currently under development requires a pointing accuracy of no less than 0.00034" [2]. Recently, the staring imaging system of a small satellite and an X-ray imager of a special solar observation satellite, both developed in China, have revealed high accuracy requirements for their pointing systems [3-4]. Furthermore, even the accuracy of the pointing system of China's "Mozi" quantum satellite has reached 2 μrad [5]. The photoelectric tracking and aiming

system is also the core component of the aviation fighter’s pod system, it requires the pointing system to meet the accuracy level of sub mrad, for example, the airborne laser communication’s pod adopts a composite pointing mechanism and its pointing accuracy reaches 10 μrad [6]. High-precision pointing technology is also key for photoelectric equipment for the landing guidance of carrier-based aircraft [7].

In civil applications, the cluster control of modern unmanned aerial vehicles adopts laser communication, with one of its core components being high-precision pointing systems [8]. In addition, this technology is also the core component of underwater laser communication systems [9]. Therefore, research into high-precision pointing technology still has important significance and value.

At present, only single-stage pointing systems using piezoelectric ceramic material, micro electromechanical system or flexure mechanism can achieve the performance of high-precision pointing [10-12], but their workspace is very small and their control is complex [13-14]. Therefore, current high-precision pointing technology must adopt a two-stage technology, i.e., a double stability system with a primary pointing mechanism and a secondary stability of fast mirror. However, the complexity of this two-stage system hinders its application and only recently studies reported that it has been used on satellite photoelectric equipment [15-16]. The realization of high-precision pointing on a single stage is therefore an important research direction for the future. The latest international report is that the accuracy of a single-stage pointing system has reached 80 μrad (0.004°) [17]. Under this background, we propose a concept of single-stage high-precision pointing technology and studied it through theoretical analysis and experiments. This study expounds working principle and verification results of this technology in detail. These research results lay a foundation for further research in the near future.

2 System description

2.1 Configuration

Although significant progress has been made regarding the development of high-precision pointing systems, further improving the accuracy of pointing systems remains a substantial challenge. The current two-stage pointing system has reached sub mrad accuracy but it also brings technical complexity and instability. A single-stage pointing system is proposed here, with high pointing accuracy achieved by eliminating the floating errors of the middle link of the mechanism, thereby making it a relatively simple system. The research objective of this project is that the uniaxial error is not greater than 0.005°, the spatial synthesis error is not greater than 0.008° and the load is not less than 100 kg. Considering the engineering requirements, researchers have adopted the embedded control technology and write the control software in C, with an upper computer used to simulate the instructions. The composition of this single-stage high-precision pointing system is shown in Figure 1, with the system consisting of an upper computer, a controller and a pointing mechanism. The upper computer sends pointing instructions to the controller, the controller calculates the execution parameters of the actuator according to the instructions, i.e., the output displacement of the two legs, while the position sensor feeds back the pointing position to the controller. According to the error elimination algorithm, the controller corrects the real pointing position until the target accuracy is reached.

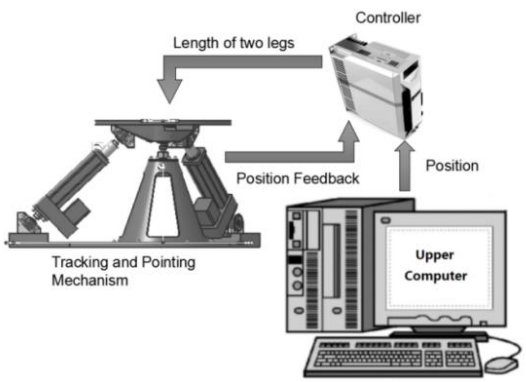

Figure 1 Configuration of high-precision pointing system

2.2 Pointing mechanism

Because of the high stiffness characteristics of the parallel mechanism [18], its transmission accuracy is better than that of the series mechanism. Therefore, researchers have proposed a two degree of freedom (DOF) parallel mechanism known as the 2RPS mechanism. This mechanism is composed of two sliding pairs Pi (i = 1,2), four ball joint pairs S_j (j = 1–4) and a cylindrical pair R_1 and its composition and principle are shown in Figures 2 and 3, respectively.

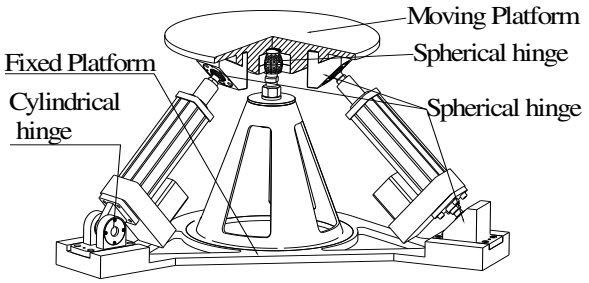

Figure 2 Composition of parallel mechanism of 2RPS

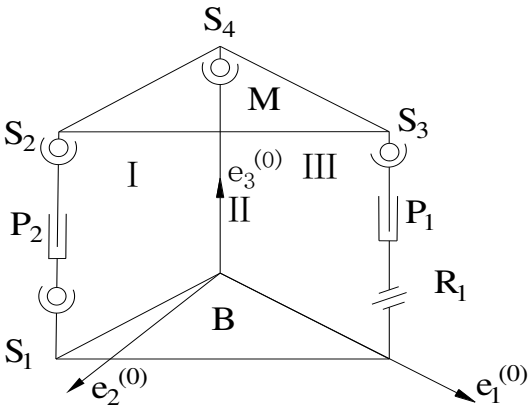

Figure 3 Graph of mechanism principle

Many opinions of the calculation method of the DOF of the spatial mechanism have been proposed but the more recognized method is to convert the spatial mechanism into the solution relationship in the plane [19-20]. Equation (1) is used to calculate the DOF of the parallel mechanism:

$$W = P_x - \lambda - 3N \tag{1}$$

where W is the number of DOFs for the spatial mechanism, P_X is the total number of DOFs for the motion pair, λ is the number of redundant DOFs for the motion pair and N is the number of closed rings of the mechanism. The pointing mechanism has three closed rings, namely, rings I, II and III, as shown in Figure 3. For ring I, its number of DOFs is W_I = 10-6-3 × 1 = 1. For ring II, its number of DOFs is W_{II} = 12-8-3 × 1 = 1. For ring III, its number of DOFs is W_{III} = 8-5-3 × 1 = 0. The number of DOFs of the pointing mechanism is $W = W_I + W_{II} + W_{III} = 2$, so the number of DOFs of the pointing mechanism meets the design requirements.

2.3 Control strategy

Only when the mechanism has an effective control strategy can it achieve optimal performance. The comprehensive errors are the main reason leading to the loss of precision of parallel mechanism [21-22]. It is necessary for researchers to study a control algorithm with error compensation. Therefore, researchers have proposed a control strategy with error elimination as the core goal, as shown in Figure 4.

The upper computer gives the expected pointing vector $\boldsymbol{n}_{exp}$ and then a controller solves the vector $\boldsymbol{n}_{exp}$, so the vector $\boldsymbol{p}_{exp}$ of the two legs is obtained when the solution is completed. The controller adjusts the two legs according to the calculated value. An ultra-high-precision position sensor collects the data of the real positions, which is expressed as a vector $\boldsymbol{n}_{true}$. There must be a difference between $\boldsymbol{n}_{true}$ and $\boldsymbol{n}_{exp}$ and the difference is the pointing error, which is defined as $\mu_{error} = \left|\boldsymbol{n}_{true} - \boldsymbol{n}_{exp}\right|$. If the pointing error is greater than 0.005 °, the controller will continue to adjust the mechanism. When the error is less than 0.005 °, the pointing mechanism will stop pointing，so an error elimination algorithm is necessary.

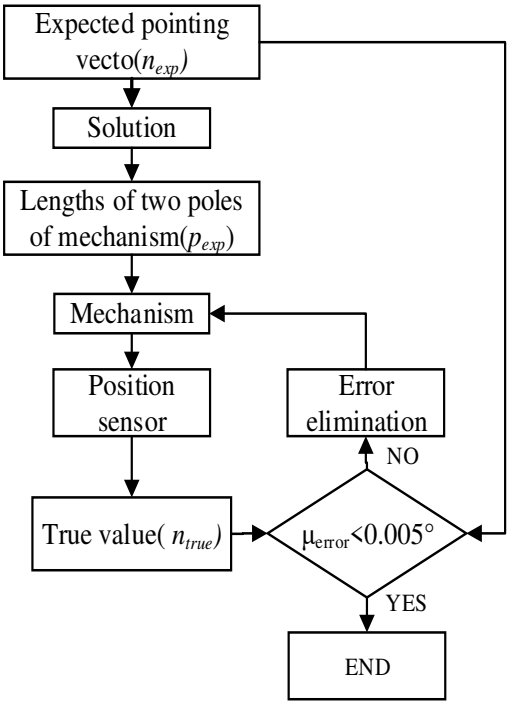

Figure 4 Process of control

Researchers have proposed an error elimination algorithm known as the double model comparison method. Its principle is to establish a theoretical model that is used as a standard to verify the error of the output position of the real mechanism and the error band is set as $\mu_{error} \le \pm 0.005^{\circ}$. The controller adjusts the leg's vector $\boldsymbol{p_{cor}}$ until the error is within the error band and then the pointing system stops. The flow of this error elimination algorithm is shown in Figure 5. According to the control strategy, the solution model of the pointing system is composed of a reverse solution model and a forward solution model.

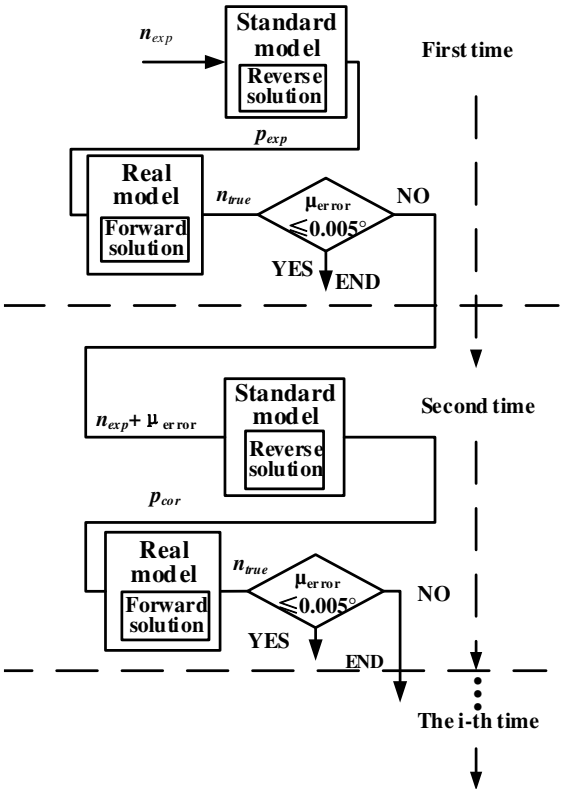

Figure 5 Process of error elimination algorithm

3 Kinematic model and its simulation

3.1 Kinematic reverse solution model

The reverse solution model is an algorithm to obtain the input parameters of the mechanism, which are the vector parameters of the two legs obtained from the instructions. First, the spatial coordinate system is established according to the space geometry [23-24], the coordinate base $\boldsymbol{e^{(0)}}$ is set at the center point of the fixed platform of the mechanism and the intersection plane of its $\boldsymbol{e_1^{(0)}}$ (X axis) and $\boldsymbol{e_2^{(0)}}$ (Y axis) passes through the center position of the spherical joint and cylindrical joint, while the coordinate base $\boldsymbol{e^{(1)}}$ is set at the center point of the moving platform and the pointing vector $\boldsymbol{n}$ is overlapped with $\boldsymbol{e_3^{(1)}}$. The definition of the spatial coordinate system is shown in Figure 6. The superscript of the vector in this study represents the serial number of the coordinate base.

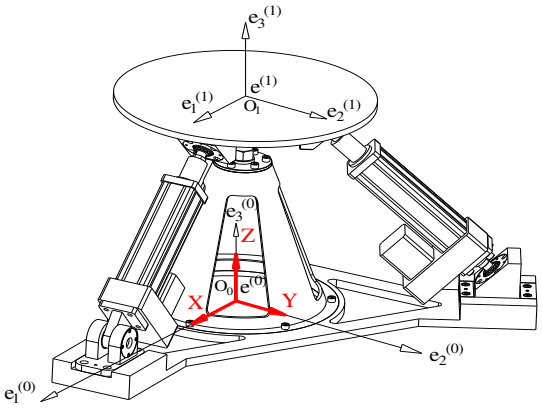

Figure 6 Definition of spatial coordinate system

The vector definition of a single leg is shown in Figure 7. $\boldsymbol{a}_i^{(0)}(i=1,2)$ are the vectors that point to the hinge S_1 or R_1 from O_0, $\boldsymbol{b}$ is the vector that points to the hinge S_4 from O_0, $\boldsymbol{d}_i(i=1,2)$ are the vectors that point to the hinge S_2 or S_3 from O_1, $\boldsymbol{c}_i(i=1,2)$ are the vectors that point to hinge S_2 or S_3 from O_0. Legs are defined as vector $\boldsymbol{p}_i(i=1,2)$ and the symbol i is the number of legs. The number of the leg, which attaches to R_1, is equal to 1.

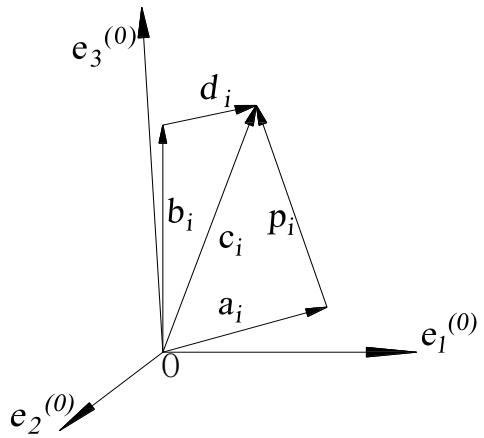

Figure 7 Vector definition of single leg

According to the space geometry and the vector definition of Figure 7, the following equations are obtained:

$$\boldsymbol{a}_i^{(0)}+\boldsymbol{p}_i^{(0)}=\boldsymbol{c}_i^{(0)} \tag{2}$$

$$\boldsymbol{b}_i^{(0)}+\boldsymbol{d}_i^{(0)}=\boldsymbol{c}_i^{(0)} \tag{3}$$

so the vector $\boldsymbol{d}_i^{(0)}$ is formulated as follows:

$$\boldsymbol{d}_i^{(0)}=\boldsymbol{a}_i^{(0)}+\boldsymbol{p}_i^{(0)}-\boldsymbol{b}_i^{(0)} \tag{4}$$

Because the vector $\boldsymbol{p}_1^{(0)}$ connects the fixed platform by a cylindrical hinge and $\boldsymbol{e}_1^{(1)}$ is in the XZ plane of base $\boldsymbol{e}^{(0)}$, the vector $\boldsymbol{d}_1^{(0)}$ is overlapped with $\boldsymbol{e}_1^{(0)}$. The pointing vector $\boldsymbol{n}$ intersects with three axes of coordinate base $\boldsymbol{e}^{(0)}$, the intersection angles are θ_x, θ_y and θ_z, respectively, so the vector $\boldsymbol{n}$ can be written as $\left[c\theta_x \quad c\theta_y \quad c\theta_z\right]^T$, where c is the cosine function. The direction of vector $\boldsymbol{n}$ is perpendicular to the plane of the moving platform, that is, the directions of $\boldsymbol{n}$ are the same as $\boldsymbol{e}_3^{(1)}$ and they all are unit vectors.

The vector $\boldsymbol{d}_1^{(0)}$ is expressed as $\left[d_{11} \quad 0 \quad d_{13}\right]^T$ and its constraint condition is given as follows:

$$\begin{cases}\boldsymbol{d}_1^{(0)}\cdot\boldsymbol{n}=0\\ \left|\boldsymbol{d}_1^{(0)}\right|=|d|^2\end{cases} \tag{5}$$

Since the moving platform will not rotate around $\boldsymbol{e}_3^{(0)}$ and $d_{11}>0$, equation (5) can be converted to the following:

$$\begin{cases}d_{11}=\dfrac{c\theta_z}{\sqrt{c\theta_z+c\theta_x}}\cdot|d|\\ d_{13}=-\dfrac{c\theta_x}{\sqrt{(c\theta_z)^2+(c\theta_x)^2}}\cdot|d|\end{cases} \tag{6}$$

The vector $\boldsymbol{d}_2^{(0)}$ is obtained by rotating $\boldsymbol{d}_1^{(0)}$ around $\boldsymbol{n}$. The rotation formula is $\boldsymbol{d}_j^{(0)}=\boldsymbol{A}_n\cdot\boldsymbol{d}_i^{(0)}$ and its conversion matrix is equation (7), where **c** is a cosine function, **s** is a sinusoidal function and the angle α is equal to 120°. The vector $\boldsymbol{p}_i^{(0)}$ can be calculated by $\boldsymbol{p}_i^{(0)}=\boldsymbol{d}_i^{(0)}+\boldsymbol{b}^{(0)}-\boldsymbol{a}_i^{(0)}$, where $\boldsymbol{a}_i^{(0)}$ and $\boldsymbol{b}^{(0)}$ are known.

$$\boldsymbol{A}_n=\begin{bmatrix} n_1^2(1-c\alpha)+c\alpha & n_1\cdot n_2(1-c\alpha)-n_3\cdot s\alpha & n_1\cdot n_3(1-c\alpha)+n_2\cdot s\alpha\\ n_1\cdot n_2(1-c\alpha)+n_3\cdot s\alpha & n_2^2(1-c\alpha)+c\alpha & n_2\cdot n_3(1-c\alpha)-n_1 s\alpha\\ n_1\cdot n_3(1-c\alpha)-n_2 s\alpha & n_2\cdot n_3(1-c\alpha)+n_1 s\alpha & n_3^2(1-c\alpha)+c\alpha \end{bmatrix} \tag{7}$$

3.2 Kinematic forward solution model

Contrary to the reverse solution model, the forward solution model deduces the pointing vectors from the values of the two legs. Figure 8 shows a vector diagram

with two legs. The vector from the spherical joint of S_3 to S_2 is expressed as $\boldsymbol{f}$ and the other vectors are defined as shown in Figure 7.

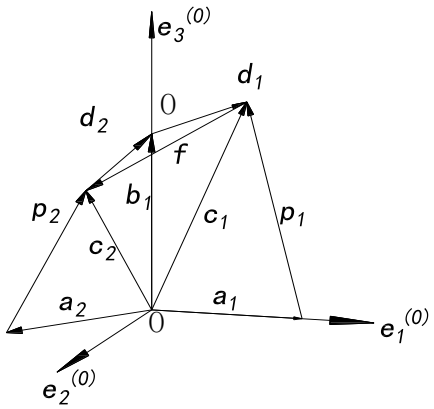

Figure 8 Vector graph of double legs

As shown in Figure 8, the lengths of $\boldsymbol{p}_i^{(0)}$ (i = 1,2) are p1 and p2 and the lengths of vectors $\boldsymbol{a}_i^{(0)}$, $\boldsymbol{b}^{(0)}$ and $\boldsymbol{d}_i^{(0)}$ are a, b and d, respectively. The vector $\boldsymbol{c}_1^{(0)}$ is expressed as $\begin{bmatrix} c_{11} & 0 & c_{13} \end{bmatrix}^T$ and finally the equation for solving the elements of $\boldsymbol{c}_1^{(0)}$ is obtained as follows:

$$\begin{cases} c_{11}^2 + (c_{13} - b)^2 = d^2 \\ c_{13}^2 + (c_{11} - a_{11})^2 = p_1^2 \end{cases} \tag{8}$$

The vector $\boldsymbol{c}_2^{(0)}$ and $\boldsymbol{f}$ are expressed as $\begin{bmatrix} c_{21} & c_{22} & c_{23} \end{bmatrix}^T$ and $\begin{bmatrix} c_{11} - c_{21} & -c_{22} & c_{13} - c_{23} \end{bmatrix}^T$, respectively, the length of $\boldsymbol{f}$ is known as f, so the elements of $\boldsymbol{c}_2^{(0)}$ can be solved by:

$$\begin{cases} c_{21}^2 + c_{22}^2 + (c_{23} - b)^2 = d^2 \\ (c_{21} - a_{21})^2 + (c_{22} - a_{22})^2 + (c_{23} - a_{23})^2 = p_2^2 \\ (c_{11} - c_{21})^2 + c_{22}^2 + (c_{13} - c_{23})^2 = f^2 \end{cases} \tag{9}$$

The vector $\boldsymbol{d}_1^{(0)}$ and $\boldsymbol{d}_2^{(0)}$ are defined by $\boldsymbol{d}_i^{(0)} = \boldsymbol{c}_i^{(0)} - \boldsymbol{b}_i^{(0)}$, so the pointing vector can be solved by $\boldsymbol{n} = \boldsymbol{d}_1^{(0)} \times \boldsymbol{d}_2^{(0)}$.

3.3 Simulation results

The simulation program of the mathematical model was compiled using MATLAB software. The parameters of the pointing mechanism are shown in Table 1. Because the accuracy of parameter $|\boldsymbol{b}|$ is difficult to guarantee in engineering, we set the error range of $|\boldsymbol{b}|$ as 5 mm in the calculation program and then calculated the workspace and pointing error of the pointing system.

Table 1 Parameters of the pointing mechanism

$\lvert\boldsymbol{a}\rvert$ （mm）	$\lvert\boldsymbol{b}\rvert$ (mm)	$\lvert\boldsymbol{d}\rvert$ (mm)	α (°)
388	376.9	135.6	120

Figure 9 shows the simulation result of the workspace of the mechanism and its workspace is ± 9° for two axes. The calculation results of the pointing error are shown in Figures 10 and 11. It can be seen from these figures that the uniaxial accuracy of the system is >0.0012° and the spatial synthetic pointing accuracy is >0.002°.

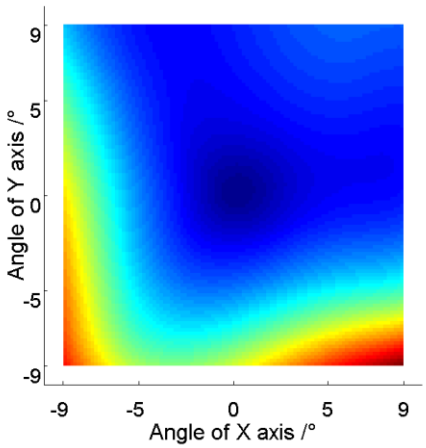

Figure 9 Simulation results of mechanism workspace

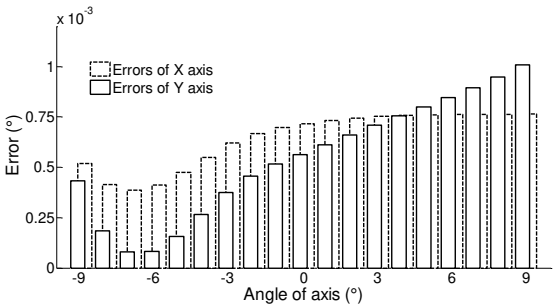

Figure 10 Simulation results of uniaxial accuracy

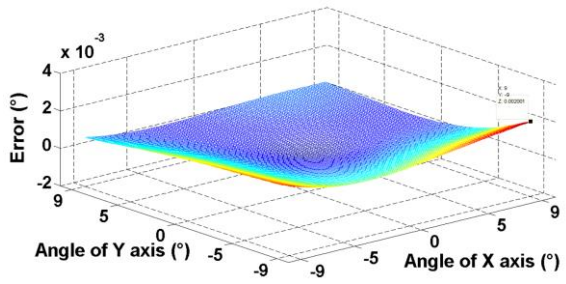

Figure 11 Simulation results of synthetic pointing accuracy

4 Verification and analysis of results

4.1 Verification

In order to further verify the correctness of this scheme, we manufactured a prototype, as shown in Figure 12.

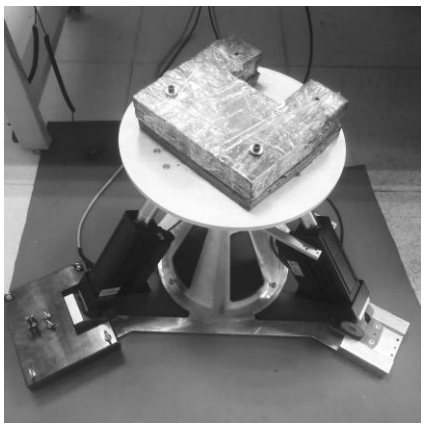

Figure 12 Photograph of principle prototype

First, the workspace of the pointing system was tested and the upper computer gives the direction instructions of two axes at an interval of 3°. The position sensor obtains the data of the two axes of the pointing mechanism and these data are shown in Figure 13. It can be seen that the workspace of the mechanism meets the requirement of ±9° for the two axes.

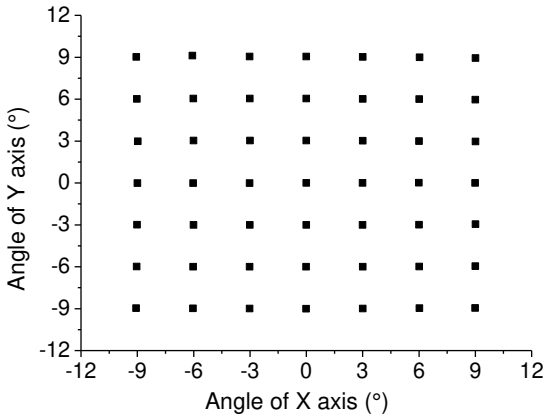

Figure 13 Test results of workspace

We tested the uniaxial error loaded with 0 and 110 kg, respectively, and the results are shown in Figure 14. The test results show that the uniaxial error of this pointing system is <0.004° even under the load condition. We also tested the spatial synthetic pointing error of the pointing system and the test results are shown in Figure 15. The synthetic spatial pointing error is <0.006°.

The response speed is also an important parameter to evaluate the pointing system. Generally, the mechanical system will have an adjustment process in the working position. The adjustment time is known as the pointing stability time for the high-precision pointing system and when the stability time of the system is shorter, its response characteristics are better. The researchers tested the stability time of the prototype when the control error band was set as ±0.005° and Figure 16 presents the test results. It can be seen from the data that the stability time of the prototype is <100 ms.

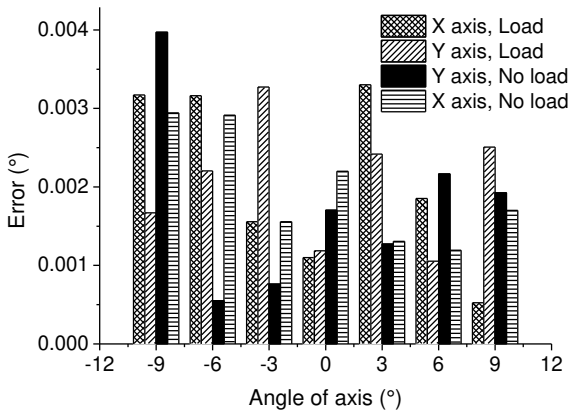

Figure 14 Test results of uniaxial error

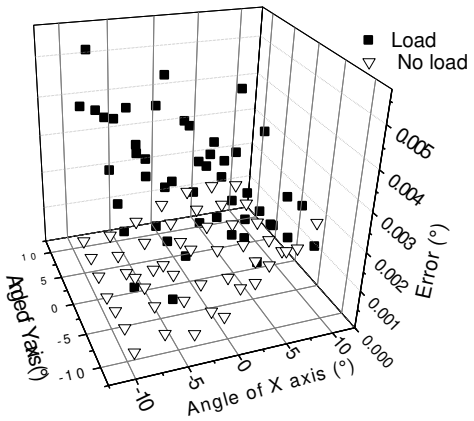

Figure 15 Test results of synthesis error

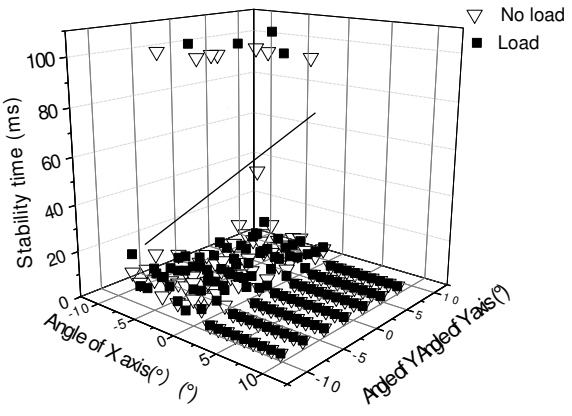

Figure 16 Test results of stability time

4.2 Analysis of results

The prototype is one of the achievements in the study. The research objective of this project is the uniaxial error is not greater than 0.005° , the synthesis error is not greater than 0.008° and the load is not less than 100 kg. The experimental results of the prototype have reached these properties, and the prototype performs satisfactorily. The experimental results are analyzed as follows.

（1） This pointing system used a 2-DOF parallel mechanism, which has a workspace of ±9° for two axes with the parameters given in Table 1. The data also show that the mechanism has no singular positions in the workspace.

（2） The uniaxial error of the single-stage pointing system is <0.004° and its spatial synthesis error is <0.006°. These values are higher than the simulation results. In the test, the researchers observed that the vibration will cause significant disturbance to the test and studies have also proved the impact of vibration on the pointing accuracy [25], so the vibration of the test environment may lead to this difference. The pointing error with load is higher than that without load, and the data with load is also more discrete than the simulation results, which are all due to the discreteness caused by the inertia of load.

（3） The stability time of the pointing system is insensitive to the load. Under the two load states, most of the test values are within 30 ms and only a few values are near 100 ms. Moreover, the data under the two load states are relatively consistent, which shows that the error elimination algorithm plays a good role.

5 Conclusions

The researchers put forward a scheme of high-precision pointing technology in the study, and it adopts an idea of no position floating. The researchers has developed a prototype for proving the idea, which has no floating errors of transmission, and it erased the cumulative errors. This idea can simplify the control algorithm. Even if there is the influence of clearance in the ball hinges [26], the study still achieves the research goal. The main conclusions are as follows:

（1） In order to reduce the complexity of the pointing system, a single-stage high-precision pointing technology is proposed. When the prototype of this scheme is loaded with 110 kg, its synthesis error is still no more than 0.006°, its stability time is no more than 100 ms and its workspace is ±9° for two axes, so we have achieved the expected goal.

（2） Eliminating the floating errors of the middle link of the pointing mechanism can effectively improve the pointing accuracy, based on this design idea, we have developed a new 2RPS parallel pointing mechanism and an error correction algorithm. The theoretical and

experimental results proved the correctness of this scheme.

（3） In the test, it is found that the vibration has caused significant disturbance to the results; this is because there is no vibration suppression device in the prototype. If the vibration suppression technology is added to the scheme, the pointing accuracy and stability can be further improved, which has also become an important aspect for further research in the future.

（4） The high-precision pointing technology proposed in this study is a single platform and the test also proves that this scheme is correct and realizable. Therefore, the research results of this study can effectively reduce the complexity of the existing pointing technology, so as to provide a method for the compact and lightweight of the system in the future.

Acknowledgements

We thank International Science Editing (http://www.internationalscienceediting.com) for editing this manuscript.

Authors' contributions

Yong-Gang Du proposed the whole research scheme and he designed and made the prototype. He wrote the manuscript. Yu-Lin Wang compile the soft and finished the simulation. Xue-Song Wang and ChunJie Yan formulated the test scheme. All authors read and approved the final manuscript.

Biographical notes

Yong-Gang Du, born in 1975, is currently a senior engineer at *Institute of Lanzhou Physics*, *China*. He received his master degree from *China Academy of Space Technology*, *China*, in 2006. His research interests include mechanism and control, mechanism in space, extraterrestrial object sampling technology.

Tel: +86-0931-4585359; E-mail: duygemail@163.com

Yu-Lin Wang, born in 1993, is currently an engineer at *Institute of Lanzhou Physics, China.* He received his master degree from *Lanzhou University, China,* in 2018. His research interests include control and measurement, BEng computer communications.

Tel: +86-0931-4585359; E-mail: 452604267@qq.com

Xue-Song Wang, born in 1976, is a senior engineer at *Institute of Lanzhou Physics, China.* He received his master degree from *China Academy of Space Technology, China,* in 2006. His research interests include mechanism and control.

Tel: +86-0931-4585359; E-mail: wangxsemail2021@163.com

Chun-Jie Yan, born in 1973, is currently a professor at National Key Laboratory of Vacuum Technology and Physics, China. He received his master degree from China Academy of Space Technology, China, in 2003. His research interests include vacuum technology and measure.

Tel: +86-0931-4585359; E-mail: chunjyan@163.com

Competing interests

The authors declare that they have no competing interests.

Funding

Supported by Aerospace independent R & D Fund (Grant No. YSC0519.1)

References

[1] TE PLATE M,O'SULLIVAN B, FERRUIT P. (2018). The European optical contribution to the James Webb space telescope. Journal of Advanced Optical Technologies, 7(6),353-364.

[2] Larry D Dewell,Kiarash Tajdaran,Raymond M Bell, et al. Dynamic stability with the disturbance-free payload architecture as applied to the Large UV/Optical/Infrared(LUVOIR)mission[C]// Proceeding of SPIE.Bellingham,WA:SPIE,2017.

[3] LU Qiang. (2020). Geometric calibration method of plane array camera with 60 degrees two-dimensional pointing

mirror. Journal of Infrared and Millimeter Waves，39(3),356-362.(in Chinese)

[4] YU Fu, SU Yang, ZHANG Zhe. (2020). Research on the Solar Aspect System Algorithm of ASO-S/HXI. ACTA ASTRONOMICA SINICA,61(4),79-89. (in Chinese)

[5] Cong Shuang, Duan Shiqi. (2021). Simulation Experiment of Quantum Ranging Process Based on the "Mozi" Quantum Satellite. Journal of System Simulation,33(2),377-388.(in Chinese)

[6] MENG Li-xin, ZHAO Ding-xuan, ZHANG Li-zhong. (2015). The Test of Tracking Accuracy and Design of Airborne Laser Communication Stabilized Pod. Acta Armamentarii, 36(10),1916-1923.(in Chinese)

[7] GE Bin，GAO Huibin，YU Yi. (2014). LOS stabilization of optic-electro landing system. Journal of Optics and Precision Engineering，22(6), 1577-1583.(in Chinese)

[8] Qing Li, Lei Liu, Xiaofei Ma, et al. “Development of MultitargetAcquisition, Pointing,and Tracking System for Airborne Laser Communication”, IEEE RANSACTIONS ON INDUSTRIAL INFORMATICS, VOL.15, NO.3 pp.1720-1729, MARCH 2019.

[9] Fangbo Qin, Dapeng Zhang, Dengpeng Xing. Demonstration of vehicle-to-vehicle optical pointing,acquisition,and tracking for undersea laser communications Free-Space Laser Communications, Proc. of SPIE 10910 Free-Space Laser Communications XXXI,109100Z, 4 March 2019.

[10] Yagiz Kaymak. A Survey on Acquisition, Tracking, and Pointing Mechanisms for Mobile Free-Space Optical, IEEE COMMUNICATIONS SURVEYS & TUTORIALS, VOL. 20, NO. 2, SECOND QUARTER 2018.

[11]Muhammad ABID, Jingjun YU, Yan XIE. (2020). Conceptual design, modeling and compliance characterization of a novel 2-DOF rotational pointing mechanism for fast steering mirror. Chinese Journal of Aeronautics, 33(12),3564-3574.

[12]Hai HUANG, Xintao ZHENG, Weipeng LI. (2019). Design and feedforward control of large-rotation two-axis scan mirror assembly with MEMS sensor integration. Chinese Journal of Aeronautics, 32(8),1912-1922.

[13] Fangbo Qin, Dapeng Zhang, Dengpeng Xing, et al. “Laser Beam Pointing Control With Piezoelectric Actuator Model Learning”, IEEE TRANSACTIONS ON SYSTEMS, MAN, AND CYBERNETICS: SYSTEMS, VOL. 50, NO. 3, pp.1024-1034, MARCH 2020.

[14] LIU Fan, ZHOU Jinxiong, MA Xiaofei. (2020). Electro-mechanical Coupling Analysis of Piezoelectrically Driven Six-degree-of-freedom Pointing Platform. JOURNAL OF MECHANICAL ENGINEERING, 56(7):10-15.(in Chinese)

[15] YAN Nanxing, LIN Zhe, LIU Yaning. (2021). Research on satellite optical axis compound pointing control method. Chinese Space Science and Technology，41(3):114-122.(in Chinese)

[16] FENG Tiantian, GAO Jingmin. (2020). A high accuracy pointing control method for space target. Chinese Space Science and Technology, 40(2):1-9.(in Chinese)

[17] Air Navigation and Electro-optics, product specification Revision . Available from: https://www.iai.co.il/.

[18] JIN Y, CHANAL H, PACCOT F. (2015). Parallel robots. Longdon: Springer.

[19] OuYang FU, YanHua LIU, DongMing SUN. (2003). EXPLORATION ON REBUIDING THE CALCULATION FORMULAR OF DEGREE OF FREEDOM OF SPACE MECHANISM. Chinese Journal of Mechanical Engineering, 39(1):60-64. (in Chinese)

[20] Zheng Huang. (2011). The degree of freedom of mechanism. Beijing:Science Press.

[21] Quan Liu, Sheng Nan Lu, Xi Lun Ding. (2018). An Error Equivalent Model of Revolute Joints with Clearances for Antenna Pointing Mechanisms. Chinese Journal of

Mechanical Engineering. doi:10.1186/s10033-018-0233-6.

[22]Liu H, Huang T, Chetwynd DG.(2011). A general approach for geometric error modeling of lower mobility parallel manipulators. Journal of Mechanisms and Robotics, 3(2):1-13.

[23] YanZhu Liu, ZhenKuan Pan, XingSheng Ge. (2016). Dynamics of Multibody Systems (Second Edition). Beijing: Higher Education Press.

[24] JiCheng Li, ZhanXian Wei. (2019). Linear Algebra and Analytic Geometry (Third Edition). Beijing: Higher Education Press.

[25] LI Lin， YUAN Li ，WANG Li. (2020). Influence of micro vibration on measurement and pointing control system of high-performance spacecraft from Hubble Space Telescope. Optics and Precision Engineering, 28(11),2478-2487. (in Chinese)

[26]Xiulong Chen, Mengqiang Cui. (2021). Dynamic Modeling and Analysis of 4UPS-UPU Spatial Parallel Mechanism with Spherical Clearance Joint. JOURNAL OF HARBIN INSTITUTE OF TECHNOLOGY(NEW SERIES), 28(3),61-78.